Contact Sensing from Force Measurements

Antonio Bicchi *
J. Kenneth Salisbury
David L. Brock

Massachusetts Institute of Technology
Artificial Intelligence Laboratory
545 Technology Square
Cambridge, MA 02139

Abstract

This paper addresses contact sensing, i.e. the problem of resolving the location of a contact, the force at the interface and the moment about the contact normals is presented. Called "intrinsic" contact sensing for the use of internal force and torque measurements, this method allows for practical devices which provide simple, relevant contact information in practical robotic applications. Such sensors have been used in conjunction with robot hands to identify objects, determine surface friction, detect slip, augment grasp stability, measure object mass, probe surfaces, control collision and a variety of other useful tasks. This paper describes the theoretical basis for their operation and provides a framework for future device design.

1 Introduction

Manipulation requires contact between a robot and an object. Although contact is the fundamental interaction which occurs in manipulation, most current robot systems do not adequately sense or use contact information. Instead,

*Antonio Bicchi is now with the Department of Electric Systems and Automation (DSEA) and Centro "E. Piaggio", Universitá di Pisa, via Diotisalvi,2, 56125 Pisa, Italia. Fax: 39-50-555636. Email: bicchi@icnucevm.cnuce.cnr.it

they rely on precisely pre-positioned objects and joint information to guide the robot into contact with these objects. As we move toward more general forms of manipulation in less structured environments, robots must rely on sensory (and ultimately perceptual) feedback. In many situations vision is a viable source of feedback about task states. However, when contact occurs, as in grasping and pushing operations, more precise and intrinsically mechanical information is required about the contact. The traditional approach to monitoring and controlling such interactions falls into two camps: force sensing and tactile sensing. The "classic" approach to force sensing employs strain sensitive elements in the wrist, drive train and other arm structures to permit measurement and control of contact and assembly forces (see Whitney [1987] for an overview). This method focuses on the net contact force and does not address contact location and geometry. On the other extreme, tactile sensors have been used to sense the details of particular contacts. Such devices employ surface mounted arrays of force sensitive elements which can be used to reveal contact locations, shapes and contact pressure distributions. See Nicholls and Lee [1989] and Howe and Cutkosky [1992] for extensive surveys of the technology.

An alternative approach, developed in detail here, relies on force and torque measurements to reveal a contact's location and force components. One of the simplest embodiments of this concept is shown in figure 1. By measuring the moment m and the force f at the fixed end of the cantilever beam, both the position of a single contact and the magnitude of its normal component of force can be found as: $p = f$ and $c = m/f$. A two dimensional version of this idea permits contact location and normal force measurement on a plane by simply measuring the force normal to the plane and two moments in the plane. One embodiment of this idea was patented by Peronneau [1972]. It turns out that it is also possible to sense the location and force components of contacts occurring on a non-planar body, under appropriate assumptions. Minsky [1972] mentions this idea in conjunction with a force sensing wrist on a robot.

Salisbury [1984] and Brock and Chiu [1985] described a structural and mathematical solution appropriate for robot fingertips that sense the location of point contacts which transmit pure forces, along with the components of the contact forces themselves. Their approach has been reconsidered by Tsujimura and Yabuta [1988]. Okada [1990] presented a suspension-cell based tactile sensor, very close in spirit to this sensing concept. Bicchi [1989, 1990a] derived a complete solution which takes into account soft-finger contact effects. Eberman and Salisbury [1989] describe how joint torque measurements in a robot arm may be used to determine the location of a contact on its links. The broad applicability of this concept warrants closer examination of the underlying mathematics and has thus motivated this paper.

This type of force-based contact sensing is inherently different from more traditional tactile sensing. The goal of most tactile sensing systems is to measure the pressure distribution over the area of contact in order to infer details about contact location and shape. However, the goal of force-based contact sensing is

to measure the net force acting on a body and to use this data to determine the properties of the contact through which the force is exerted. Since these sensors rely on measurements taken by sensing elements which are placed inside, rather than spread over, the contacting surface, they are also referred to as intrinsic tactile sensors.

Although the theory behind such sensors is relatively complex, in practice they are quite simple to build and utilize, while they offer enormous potential for improving robot manipulation dexterity. In this paper we present the theoretical aspects of intrinsic contact sensing as a basis for device design and application. In section 2, we survey three basic contact models: the *point contact without friction*, *point contact with friction* and *soft finger contact*. The soft finger contact type is particularly important, since it describes the most common situation encountered in manipulation. In section 3, we address the basic mathematics and mechanics of contact sensing, and discuss when it is possible for a sensor to determine the location and the resultant force and moment of a contact given internal force and moment measurements. Sections 6, 4, and 5 describe algorithms to solve the contact sensing problem. Section 4 presents a general, yet approximate, closed-form algorithm, section 5 describes a closed-form, exact solution for a number of simple sensor surfaces, and section 6 introduces a general iterative method. Section 7 describes some possible generalizations of the idea and finally, in section 8, numerical experiments are used to discuss the properties of the proposed algorithms. The appendix contains proofs of the propositions introduced in the text.

2 Contact Types

The concept of contact *type* is basic to understanding force-based contact sensing. The contact type establishes constraints on the forces which may be applied through the contact between two bodies [Mason and Salisbury, 1985].

If the forces which act upon a body sum to zero, it is said to be in a state of static equilibrium. These forces may arise from actuators, body forces and contacts with the environment. Although the net force and moment on a system in static equilibrium will sum to zero, there will be non-zero internal forces (i.e. structural stresses, contact forces etc.). If measurements of some of the internal forces can be made, they can be checked for consistency with the expected effects of a particular load type, and hence can be used to deduce information about the contact(s).

When arbitrary forces and moments can be transmitted through the contact (i.e. a *glued contact* type), not much may be said about the contact geometry given force measurements. However, common contact types impose constraints on the transmitted forces, in that their components are either unidirectional or limited by the friction cone. It is these constraints which make the intrinsic contact sensing practical.

A *point contact without friction* constrains the force applied to the body to be normal to the surface at the point of contact, and the moment to be zero. There are only 3 unknowns: the 2 contact coordinates and the force magnitude, so ideally only 3 independent force measurements would be required to reveal the contact location and force. If we precisely measure all 3 force components acting on the body, the associated wrench axis is a line which passes through the point of contact and is normal to the surface at that contact point[1].

A *point contact with friction* also constrains the force applied to the body to be a pure force, but it is no longer constrained to have a line of action normal to the surface at the point of contact. Since there are now 5 unknowns: the 2 contact coordinates and the 3 contact force components, ideally only 5 independent force measurements are required to measure the contact location and force components. Again, if precise measurements are available, the associated wrench axis is a line which passes through the point of contact.

Finally, if the bodies are compliant, finite portions of the surface may come into contact, and if friction is present, torques may also be exerted. In this situation, often referred to as a *soft finger contact*, the wrench axis no longer necessarily passes through the contact location. We will show below that it is possible to define and solve for the contact location, and force and moment components even in this rather general case.

2.1 Soft Finger Contact and the Contact Centroid

The soft finger contact type is the most general case among those considered above and to which intrinsic contact sensing can be applied. Point contacts with or without friction are particular cases of soft finger contacts. Indeed, this type of contact is also the most common in practical manipulation. For example, contacts through which humans manipulate objects are frequently of this type.

A soft finger contact occurs between two real (non-rigid, possibly inelastic) bodies mutually transmitting a distribution of contact tractions[2] over a finite area of contact. The tractions are assumed to be *compressive*, that is, to point at the interior part of the body (adhesive forces between bodies are therefore disregarded by this model). Because of their distributed nature, a complete characterization of contact related phenomena would involve complex continuum mechanics relationships, whose computation (if at all possible) is far beyond the capabilities of a real-time robot sensory and control system. A compact characterization of contact is necessary to render the sensing problem tractable. The traditional approach to tactile sensing consists of spatially sampling the traction distribution, and is usually limited to sensing only normal force components. A more drastic compression of data is obtained by force-based contact sensing, which provides a reduced set of contact features, useful for manipulation control. This is achieved by use of *equivalent sets* of forces. Roughly speaking, two sets of forces are equivalent if their large-scale effects are the same. The unknown distribution of contact tractions can be substituted

with an equivalent force and moment, comprised of a *resultant force* (henceforth designed with the vector $\mathbf{p}$), and a *resultant moment*, $\mathbf{q}$. To completely describe the set of forces, a point must be provided through which the resultant force is applied. The choice of this point is not trivial in the soft finger case, because contact occurs over a whole area. We show in what follows that a very convenient point to use for representing soft finger contacts is the *contact centroid*, which we define as follows:

Definition 1: Contact Centroid

Given a surface S with an outward normal direction defined everywhere on it, and a distribution Δ of compressive tractions applied on it, a contact centroid for S and Δ is a point on S such that a set of forces equivalent to Δ exists, having the following characteristics:

1. it is comprised of only a force and a torque;
2. the force is applied at that point, and is directed into S;
3. the moment is parallel to the surface normal at that point.

A contact centroid has some very useful properties, that render it a desirable point to sense. First, if contact occurs at a single point, the contact centroid coincides with that point. Thus, from force/torque measurements we obtain the contact location — a typical tactile sensing goal. Second, even if multiple points and/or finite areas are in contact, the contact centroid still contains useful geometric information, as articulated below.

Proposition 1: Property of Contact Centroids

Consider a deformable body, whose undeformed surface S is convex, and assume that a distribution Δ of compressive contact tractions is exerted on it. Consider a plane P that divides the surface of the body in two portions, confining every contact point in one half-space (see figure 2). Consider the projection of each contact point on P along the direction of the traction applied at the contact point itself. If all such projections are internal to the undeformed surface S, then the contact centroid lies on the same side of P where Δ is applied[3].

The proof of this property takes a few steps, and is presented in Appendix 1. The significance of this property is related to the fact (to be proved shortly) that it is possible to give an expression of the contact centroid in terms of force/torque measurements only. Although an intrinsic contact sensor is not able to provide an *image* of the actual contact points, we have an idea about the contact distribution since the contact points are required to "lie around" the contact centroid given appropriate constraints on surface curvature, deformability and friction (see figure 2).

As a corollary to the property above, consider a generic compressive distribution Δ, whose tractions comply with Coulomb's friction law. Given the assumptions as described in proposition 1, it is required that the projection of every friction cone on the plane P is inside the sphere S. Suppose we had a spherical sensor with a coefficient of friction $\mu = \tan\varphi$. Then the hypotheses of proposition 1 are satisfied if every contact point falls within a cone of angle $\theta = \pi - 2\varphi$, as illustrated in figure 3a. In other words, if the contact area is "small" enough, then the contact centroid is a meaningful datum to calculate. For example, suppose a spherical sensor is pressed into a corner whose walls form an angle α and whose surface friction is given by φ. Then the conditions for the viability of the contact centroid are satisfied when $\alpha > 2\varphi$.

3 Problem Formulation

One possible implementation of a contact sensor consists of a surface, which we will call a *fingertip*, attached to a six axis force/torque sensor. The force/torque sensor measures all three components of both the resultant force $\mathbf{f}$ and the resultant moment $\mathbf{m}$ with respect to the reference frame B, as shown in figure 4. Note that the choice of the reference frame B is arbitrary, since we can easily express $\mathbf{f}$ and $\mathbf{m}$ in terms of any other coordinate frame fixed to B.

The fingertip surface can be described by the implicit relation

$$S(\mathbf{r}) = 0, \tag{1}$$

where $\mathbf{r}$ is a point in space defined with respect to B. The surface S should have continuous first derivatives, so that a normal unit vector can be defined at every point on S as

$$\mathbf{n} = \frac{\nabla S(\mathbf{r})}{||\nabla S(\mathbf{r})||},$$

where ∇ indicates the gradient operator. Let $\mathbf{c}$ be the contact centroid, and $\mathbf{p}$ and $\mathbf{q}$ the force and moment applied at $\mathbf{c}$, which are equivalent to a "soft finger" contact. The measurable quantities $\mathbf{f}$ and $\mathbf{m}$ are related to the unknowns $\mathbf{c}$, $\mathbf{p}$ and $\mathbf{q}$, by force and moment balance equations,

$$\mathbf{f} = \mathbf{p}, \tag{2}$$

$$\mathbf{m} = \mathbf{q} + \mathbf{c} \times \mathbf{p}. \tag{3}$$

For soft finger contacts the torque $\mathbf{q}$ is parallel to the unit vector $\mathbf{n}$ normal to the surface at the contact centroid $\mathbf{c}$, hence

$$\mathbf{n} \propto \mathbf{q} = \frac{K}{2}\nabla S(\mathbf{c}), \tag{4}$$

for some constant K.

We call the above set of relations the *contact sensing problem*, which is stated as follows:

Definition 2: Contact Sensing Problem

Given the measurements $\mathbf{f}$ and $\mathbf{m}$, together with a surface equation $S(\cdot) = 0$, determine the location of the contact centroid(s) $\mathbf{c}$, and the related contact force $\mathbf{p}$ and moment(s) $\mathbf{q}$.

Note that, because of the definition of contact centroid, we implicitly require that $\mathbf{p}$ is compressive, i.e. directed into the surface, and that $\mathbf{q}$ is normal to S. Expanding equations 1 through 4 yields a non-linear system of ten equations in ten scalar unknowns, i.e. the nine components of $\mathbf{p}$, $\mathbf{q}$, $\mathbf{c}$, and K. However, by simply substituting equations 2 and 4 in equation 3, the problem is reduced to four equations in four unknowns. Since the problem is non-linear, we need to determine if a solution exists, and in that case if it is unique. In general, not much can be said about the existence of solutions given arbitrary $\mathbf{f}$, $\mathbf{m}$, and S, since there is no guarantee we can find an equivalent soft finger contact. A solution exists, however, if the resultant force $\mathbf{f}$ and moment $\mathbf{m}$ are measurements consistent with the effects of a soft-finger type traction distribution on a surface S.

If a solution exists, the following proposition holds about its uniqueness:

Proposition 2: Uniqueness of Solutions

A solution to the contact sensing problem is unique (if it exists), if and only if the sensor surface is convex (see proof in Appendix 2).

Proposition 1 gives conditions on Δ and S that guarantee the existence of a contact centroid. According to proposition 2, the contact centroid of a compressive distribution Δ on a convex surface is also unique.

As a final remark, the solution to equations 1 through 4 may not be trivial and a closed-form solution may not be found except for the simplest surfaces. In the following sections, we will present three methods for solving these equations.

4 Point-contact solution

The first closed-form method we present for solving the contact sensing problem utilizes more restrictive assumptions than those specified above. In particular, we assume the local torque $\mathbf{q}$ about the contact normal is zero. In other words we assume the contact model is a *point contact with friction*, as described in section 2. This assumption can lead to good results and a simple solution for a large number of practical cases. The *wrench axis* of the force system is given by

$$\mathbf{r} = \mathbf{r}_0 + \lambda \mathbf{f}, \tag{5}$$

where

$$\mathbf{r}_0 = \frac{\mathbf{f} \times \mathbf{m}}{\|\mathbf{f}\|^2}. \tag{6}$$

The wrench axis is a line through $\mathbf{r}_0$ and parallel to $\mathbf{f}$, parameterized by λ. This line intersects the convex surface S in at most two locations: one corresponding to a force pulling out of the surface and one corresponding to a force pushing into the surface. Since we do not allow adhesive forces, we can determine the contact centroid as the intersection point, for which the contact force is directed into the surface, that is

$$\mathbf{f}^T \mathbf{n}(\mathbf{c}) < 0. \tag{7}$$

When the local torque $\mathbf{q}$ is not zero, the point found by this method differs from the contact centroid. Therefore we will denote with $\mathbf{c}'$ the vector found using this (so-called "wrench-axis" or "point-contact") method.

Note that the assumption $\mathbf{q} = 0$ can be checked out directly from force/torque measurements by means of the equivalent relationship $\mathbf{f}^T \mathbf{m} = 0$. It should be pointed out that the point $\mathbf{c}'$ does not have any of the properties of contact centroids, so that it could in principle lie far away from the actual location of the contact area. Yet, point $\mathbf{c}'$ retains a valuable meaning in real conditions as an easy-to-compute approximation of the contact centroid. In order to give an estimate of the distance between $\mathbf{c}'$ and the contact centroid $\mathbf{c}$, let $\mathbf{e}$ represent the difference vector $\mathbf{e} = \mathbf{c}' - \mathbf{c}$. Suppose two sets of forces, $\mathbf{p}$ and $\mathbf{q}$ applied at $\mathbf{c}$, and $\mathbf{p}$ and $\mathbf{t}$ applied at $\mathbf{c}'$, are both equivalent with the actual set of contact forces, hence they are equivalent with each other. The balance equation of moments about $\mathbf{c}$ can be written as

$$\mathbf{q} = \mathbf{t} + \mathbf{e} \times \mathbf{p}.$$

Such a vector equation is solved by any $\mathbf{e}$ of the form

$$\mathbf{e} = \frac{(\mathbf{q} - \mathbf{t}) \times \mathbf{p}}{\|\mathbf{p}\|^2} + \nu\, \mathbf{p}. \tag{8}$$

Recalling that, after the definition of wrench axis, $\mathbf{t}$ is parallel to $\mathbf{p}$, and that, by definition of contact centroid, $\mathbf{q}$ is normal to the surface, we can rewrite equation 8 as

$$\mathbf{e} = \frac{\mathbf{q} \times \mathbf{p}_t}{\|\mathbf{p}\|^2} + \nu\, \mathbf{p},$$

where $\mathbf{p}_t = \mathbf{p} - (\mathbf{p}^T \mathbf{n})\mathbf{n}$ is the tangential (friction) component of the contact resultant force. Since the error vector $\mathbf{e}$ is the sum of two mutually orthogonal vectors, its length is at least as large as

$$\|\mathbf{e}\| \geq \frac{\|\mathbf{q}\|\, \|\mathbf{p}_t\|}{\|\mathbf{p}\|^2}.$$

In view of this result, it can be observed that the distance between the point found by the wrench-axis method and the contact centroid grows quickly as

friction increases. Then, the approximation of the contact centroid with point $\mathbf{c}'$ should be avoided if high-friction and/or compliant materials are employed in building the fingertips. Numerical examples are provided in the discussion section.

5 Solution for Ellipsoidal Surfaces

The main advantage of the wrench-axis method is that the contact location problem is reduced to that of finding the intersection of a line with a surface. However, this method has two major drawbacks. First, it does not provide information about the moment exerted through a soft-finger contact, and second, it only approximates the contact centroid. In this section we solve the contact sensing problem and avoid such shortcomings. However, in order to guarantee a closed-form algorithm and to simplify calculations, the fingertip surface will be restricted to belong to a specific class of surfaces, namely, quadratic forms of the type

$$S(\mathbf{r}) = \mathbf{r}^T \mathbf{A}^T \mathbf{A} \mathbf{r} - R^2 = 0, \tag{9}$$

where $\mathbf{A}$ is a constant coefficient matrix, and R is a scale factor used for convenience. Since the reference frame B can be moved arbitrarily, we can assume without loss of generality that $\mathbf{A}$ can be written in diagonal form

$$\mathbf{A} = \begin{pmatrix} 1/\alpha & 0 & 0 \\ 0 & 1/\beta & 0 \\ 0 & 0 & 1/\gamma \end{pmatrix}.$$

In order to guarantee the uniqueness of solutions, the surface specification must be further restricted to convex portions of the quadratic form (for instance, one of the sheets of a double hyperboloid would be an appropriate sensor surface). In the interest of simplicity, however, we will consider in the following only general ellipsoids (i.e., definite positive $\mathbf{A}$ matrices). In this case, the principal axes of the ellipsoid are given by $2\alpha R$, $2\beta R$ and $2\gamma R$, with $0 < 1/\alpha \leq 1$, $0 < 1/\beta \leq 1$, $0 < 1/\gamma \leq 1$.

It should be noted that ellipsoids are important for several reasons. First, ellipsoids approximate, up to the second order, any continuous convex surface. Second, very common surfaces, such as spheres, cylinders, and planes, can be regarded as limit cases of an ellipsoid. Finally, the ellipsoid assumption is standard in contact mechanics (e.g. the Hertzian theory of elastic contact).

Substituting equation 9 into equation 4 yields

$$\mathbf{n} = \frac{\mathbf{A}^2\mathbf{c}}{\|\mathbf{A}^2\mathbf{c}\|} \propto \mathbf{q} = K\mathbf{A}^2\mathbf{c}, \tag{10}$$

and substituting this and equation 2 in equation 3, we obtain

$$\mathbf{m} = K\mathbf{A}^2\mathbf{r} + \mathbf{r} \times \mathbf{f}. \tag{11}$$

Equations 9 and 11 form a system of four non-linear equations and four unknowns which can be rewritten in the form

$$\begin{aligned} \mathbf{\Gamma c} &= \mathbf{m} && (12) \\ \mathbf{c}^T\mathbf{A}^2\mathbf{c} &= R^2, && (13) \end{aligned}$$

where $\mathbf{\Gamma} = \mathbf{\Gamma}(K)$ is a 3×3 matrix whose elements are functions of K and of the measured force components f_1, f_2 and f_3,

$$\mathbf{\Gamma}(K) = \begin{pmatrix} K/\alpha^2 & f_3 & -f_2 \\ -f_3 & K/\beta^2 & f_1 \\ f_2 & -f_1 & K/\gamma^2 \end{pmatrix}.$$

The determinant of $\mathbf{\Gamma}(K)$ is given by

$$\det \mathbf{\Gamma}(K) = K(K^2D^2 + \|\mathbf{Af}\|^2),$$

where $D = \det \mathbf{A}$. The matrix $\mathbf{\Gamma}(K)$ is singular for $K = 0$, i.e. when the local torque $\mathbf{q}$ is zero. In this case (which can be detected by the simple equivalent condition $\mathbf{f}^T\mathbf{m} = 0$, as already mentioned), the contact centroid can be determined exactly by the wrench-axis method. The value of the parameter λ in equation 5 corresponding to the intersection of the wrench-axis with the ellipsoid surface is given by

$$\lambda = \frac{-\mathbf{f}'^T\mathbf{r}'_0 - \sqrt{(\mathbf{f}'^T\mathbf{r}'_0)^2 - \|\mathbf{f}'\|^2(\|\mathbf{r}'_0\|^2 - R^2)}}{\|\mathbf{f}'\|^2},$$

where $\mathbf{f}' = \mathbf{Af}$ and $\mathbf{r}'_0 = \mathbf{Ar}_0$ (recall the definition of $\mathbf{r}_0$ in equation 6).

Whenever $\mathbf{f}^T\mathbf{m} \neq 0$, $\mathbf{\Gamma}(K)$ has an inverse $\mathbf{\Gamma}^{-1}(K)$ such that, by solving equation 12 for $\mathbf{c}$, we obtain

$$\mathbf{c} = \mathbf{\Gamma}^{-1}\mathbf{m} = \frac{1}{\det \mathbf{\Gamma}}[K^2D^2\mathbf{A}^{-2}\mathbf{m} + K(\mathbf{A}^2\mathbf{f}) \times \mathbf{m} + (\mathbf{f}^T\mathbf{m})\mathbf{f}]. \tag{14}$$

By substituting equation 14 into equation 13, a scalar equation in the only unknown K is obtained as

$$\mathbf{c}^T\mathbf{A}^2\mathbf{c} = R^2 = \frac{K^4D^4\|\mathbf{A}^{-1}\mathbf{m}\|^2 + K^2\|\mathbf{A}(\mathbf{A}^2\mathbf{f} \times \mathbf{m})\|^2 + (\mathbf{f}^T\mathbf{m})^2(\|\mathbf{Af}\|^2 + 2K^2D^2)}{K^2(K^2D^2 + \|\mathbf{Af}\|^2)^2} \tag{15}$$

For such a 6-th order equation a closed-form solution should not be expected in general, due to Galois' theorem. For the particular surface assumed, though, we observe that

$$\|\mathbf{A}(\mathbf{A}^2\mathbf{f} \times \mathbf{m})\|^2 = D^2 \left[\|\mathbf{A}^{-1}\mathbf{m}\|^2\|\mathbf{A}\mathbf{f}\|^2 - (\mathbf{f}^T\mathbf{m})^2\right],$$

so that equation 15 can be simplified in a biquadratic equation as

$$K^4D^2R^2 + K^2\left[R^2\|\mathbf{A}\mathbf{f}\|^2 - D^2\|\mathbf{A}^{-1}\mathbf{m}\|^2\right] - (\mathbf{f}^T\mathbf{m})^2 = 0.$$

Only one of the four possible K solving this equation is real and consistent with the hypothesis of non-adhesive contact, and is given by

$$K = \frac{-\text{sign}(\mathbf{f}^T\mathbf{m})}{\sqrt{2}RD}\sqrt{\sigma + \sqrt{\sigma^2 + 4D^2R^2(\mathbf{f}^T\mathbf{m})^2}}, \tag{16}$$

where

$$\sigma = D^2\|\mathbf{A}^{-1}\mathbf{m}\|^2 - R^2\|\mathbf{A}\mathbf{f}\|^2,$$

and

$$\text{sign}(x) = \begin{cases} -1, & \text{for} \quad x < 0 \\ 0, & \text{for} \quad x = 0 \\ 1, & \text{for} \quad x > 0 \end{cases}.$$

By substituting back K in equation 14 and equation 10, we obtain the complete solution for $\mathbf{c}$ and $\mathbf{q}$, respectively.

5.1 Particular Cases

We will now develop solutions for some particular cases of practical importance, namely the sphere, cylinder and plane.

5.1.1 Sphere

For a spherical sensor surface of radius R centered at the origin of the force/torque reference frame B, the matrix $\mathbf{A}$ equals the identity $\mathbf{I}_3$, and $D = 1$. Hence,

$$K = \frac{-\text{sign}(\mathbf{f}^T\mathbf{m})}{\sqrt{2}R}\sqrt{\sigma' + \sqrt{\sigma'^2 + 4R^2(\mathbf{f}^T\mathbf{m})^2}}.$$

where $\sigma' = \|\mathbf{m}\|^2 - R^2\|\mathbf{f}\|^2$.

The contact centroid location (for nonzero K) is given by

$$\mathbf{c} = \frac{1}{K(K^2 + \|\mathbf{f}\|^2)}\left[K^2\mathbf{m} + K\mathbf{f} \times \mathbf{m} + (\mathbf{f}^T\mathbf{m})\mathbf{f}\right],$$

whereas, for $K = 0$, the contact centroid is found using equation 5 with

$$\lambda = -\frac{1}{\|\mathbf{f}\|}\sqrt{R^2 - \frac{\|\mathbf{f} \times \mathbf{m}\|^2}{\|\mathbf{f}\|^4}}.$$

5.1.2 Cylinder

Consider a cylinder having the axis parallel to the z axis of the sensor frame B, and circular cross section of radius R. Such surface can be described as the limit case of an ellipsoid with characteristic matrix given by

$$\mathbf{A} = \begin{pmatrix} 1 & 0 & 0 \\ 0 & 1 & 0 \\ 0 & 0 & 1/\gamma \end{pmatrix}$$

for $\gamma \to \infty$. Applying the same limit to equation 16, we have

$$K = \frac{-\mathbf{f}^T\mathbf{m}}{\sqrt{R^2\|\mathbf{f}^\perp\|^2 - \|\mathbf{m}''\|^2}},$$

where $\mathbf{f}^\perp = (f_1, f_2, 0)^T$ is the component of $\mathbf{f}$ normal to the cylinder axis, and $\mathbf{m}'' = (0, 0, m_3)^T$ is the component of $\mathbf{m}$ parallel to the same axis. If $K = 0$, the wrench method (equation 5) should be applied. Otherwise, the contact centroid on the cylindrical surface of the fingertip is given by

$$\mathbf{c} = \frac{1}{K\|\mathbf{f}^\perp\|^2}\,[K^2\mathbf{m}'' + K\mathbf{f}^\perp \times \mathbf{m} + (\mathbf{f}^T\mathbf{m})\mathbf{f}].$$

5.1.3 Plane

An ellipsoid with matrix $\mathbf{A}$ of the form

$$\mathbf{A} = \begin{pmatrix} 1/\gamma & 0 & 0 \\ 0 & 1/\gamma & 0 \\ 0 & 0 & 1 \end{pmatrix}$$

degenerates, for $\gamma \to \infty$, in a couple of parallel planes perpendicular to the x axis of B, at a distance $\pm R$ from the origin. If $\mathbf{f}'' = (0, 0, f_3)^T$ is the contact force component parallel the z axis, equations 16 and 14 become

$$K = \frac{-\mathbf{f}^T\mathbf{m}}{R\|\mathbf{f}''\|}$$

and

$$\mathbf{c} = \frac{1}{\|\mathbf{f}''\|^2}\,(\mathbf{f}'' \times \mathbf{m} + R\,\|\mathbf{f}''\|\,\mathbf{f}).$$

It should be noted that the last formula holds even with $K = 0$.

6 Iterative solution

The final method for solving the contact sensing problem is valid for any surface specification, but implies an iterative algorithm to be run at each sensor sampling time. The computational efficiency of the algorithm is therefore of utmost importance for real-time applications.

As customary when dealing with the numerical solution of vector multivariate functions, we rewrite the problem equations in the relaxation-method form

$$\mathbf{g}(\mathbf{x}) = 0, \tag{17}$$

where

$$\begin{aligned}
\mathbf{x}^T &= (x_1, x_2, x_3, x_4)^T = (\mathbf{c}^T, K/2); \\
\mathbf{g}^T(\mathbf{x}) &= (g_1(\mathbf{x}), g_2(\mathbf{x}), g_3(\mathbf{x}), g_4(\mathbf{x}))^T; \\
g_1(\mathbf{x}) &= x_4 \nabla S_1 - f_2 x_3 + f_3 x_2 - m_1; \\
g_2(\mathbf{x}) &= x_4 \nabla S_2 - f_3 x_1 + f_1 x_3 - m_2; \\
g_3(\mathbf{x}) &= x_4 \nabla S_3 - f_1 x_2 + f_2 x_1 - m_3; \\
g_4(\mathbf{x}) &= S(x_1, x_2, x_3).
\end{aligned}$$

Standard algorithms (see e.g. [Dahlquist and Björk, 1974]) for the iterative solution of such equations can be applied, perhaps the most notable being the Newton-Raphson method or its variations. The Jacobian matrix $\mathbf{G}$ associated with the problem can be evaluated as

$$\mathbf{G}(\mathbf{x}) = \frac{\partial \mathbf{g}}{\partial \mathbf{x}} = \left(\begin{array}{c|c} x_4 \mathbf{H} - \mathbf{f}_\otimes & \nabla S \\ \hline \nabla S^T & 0 \end{array} \right),$$

where $\mathbf{H}$ is the Hessian of the surface S (that is, the matrix $H_{ij} = \frac{\partial^2 S}{\partial x_i \partial x_j} \quad i, j = 1, 2, 3$), and $\mathbf{f}_\otimes$ is the cross-product matrix of $\mathbf{f}$, such that $\mathbf{f}_\otimes \mathbf{c} = \mathbf{f} \times \mathbf{c}$.

Computing $\mathbf{G}$ can be more or less time consuming, depending upon the complexity of the surface S. Computing $\mathbf{G}^{-1}$, as required by Newton-Raphson's method, can be inconvenient for real time applications. Furthermore, in this specific case, we have that $\mathbf{G}$ is singular for $x_4 = K/2 = 0$, that means that this algorithm would present serious problems whenever the contact load has very little local torque $\mathbf{q}$.

It must be noted that, in general, the numerical solution of vector multivariate nonlinear equations is not a "nice" problem (see the related comments in [Press et al., 1988]); better algorithms are available for finding the extrema of multivariate scalar functions. A possible approach to the design of an algorithm for solving equation 17 is therefore to embed the root-finding problem in a minimization one.

Since the Jacobian matrix $\mathbf{G}$ is not symmetric (its upper left minor is the sum of a symmetric and a skew-symmetric matrix), $\mathbf{g}$ cannot be straightforwardly

regarded as the gradient of some energy-like function to minimize. However, if we consider the equation

$$\mathbf{G}^T\mathbf{g}(\mathbf{x}) = 0,$$

we have that all the zeroes of $\mathbf{g}$ are also zeroes of $\mathbf{G}^T\mathbf{g}$, and $\mathbf{G}^T\mathbf{g}$ is the gradient ("potential field") associated with the positive definite scalar function $V = \frac{1}{2}\mathbf{g}^T\mathbf{g}$, whose absolute minimum is our solution.

Applying the well-known gradient descent updating law to the k-th estimate of $\mathbf{x}$, we have

$$\mathbf{x}_{k+1} = \mathbf{x}_k - \lambda\nabla V(\mathbf{x}) = \mathbf{x}_k - \lambda\mathbf{G}_k^T\mathbf{g}_k.$$

It can be observed that the application of this gradient descent technique to minimize an energy-like (Liapunov) function $V = \phi^T(\mathbf{q})\phi(\mathbf{q})$ is equivalent to the closed-loop inverse kinematic scheme proposed by Balestrino, DeMaria and Sciavicco [1984] and several others, to invert the nonlinear kinematic relationship of a robot, $\phi(\mathbf{q})$. It can be shown with a Liapunov argument that this method is locally asymptotically convergent to the desired solution, for appropriate choices of λ; and, in fact, it is intuitive that for λ (i.e. step lengths) short enough in the steepest descent direction the V function will be always kept decreasing until a minimum is reached. A discussion on the optimal choice of λ has been provided by Das, Slotine and Sheridan [1989].

The local asymptotic convergence of the algorithm means, in our current application, that the correct contact point will be found provided that the initial guess is "close enough." In order to avoid getting "stuck" at an incorrect point, is would be desirable to assess global asymptotic convergence. Unfortunately, the technique of embedding the root-finding problem in a minimization one is prone to generate such local minima, and some do exist in our specific problem even for surfaces as simple as spheres. From a practical point of view those "false" roots are easily recognized (their residues $\mathbf{g}^T\mathbf{g}$ are not zero). Moreover, if the contact being investigated changes its characteristics with continuity, starting the search from the previously obtained solution is very likely to lead to the actual solution.

7 Compound surfaces

Many applications of intrinsic contact sensing use surfaces more complex than the simple geometries described above. However, the methods presented above can be easily extended to compound surfaces made of simpler surfaces if the compound surface is convex and the component surfaces share the same normal at their boundaries. For example, the fingertip sensors of the Salisbury Robot Hand are composed of an hemisphere on top of a cylinder of equal radius, as depicted in figure 5. A solution for a compound surface is typically searched

by trial and error. The contact centroids corresponding to the given load and to the complete ellipsoids to which the basic patches of the compound surface belong, are calculated in succession. By virtue of the uniqueness property of contact centroids, the search can be stopped as soon as a contact centroid lying on the actual sensor surface is found.

If the sensor surface has sharp points, as the example depicted in figure 6, a normal direction cannot be defined at those points and the above discussed solution methods are not applicable directly. If the sensor or the object surfaces are compliant, this problem is not a major concern, since surface edges are "smoothed" out, and the properties of contact centroid guarantee that a meaningful result will be achieved anyway. However, if a rigid contact occurs on a sharp point of the sensor surface, no local torque is exerted; therefore, any point found by intersecting the wrench axis with the different surface patches should coincide with the actual contact point. Since, in general, noisy measurements are available, it may happen that no contact centroid actually lying on the sensor surface is found. In this case, a good approximation can be assumed to be the point on the sensor surface closest to the calculated centroids. The worst case is when a whole edge of the sensor surface is in contact with the object. Since local torques can be exerted, and no normal direction is defined, both methods discussed above would fail. However, the practical relevance of such cases is negligible.

More complex surfaces that do not comply with the above assumptions of convexity and regularity can be dealt with in some cases. For example, a typical manipulator arm is composed of individually convex surfaces, but is not convex as a whole (see figure 7). Ebermann and Salisbury [1989] discussed the use of joint torque measurements to infer information about contacts occurring on the last link of the robot. On the other hand, a force/torque sensor at the base of the manipulator would sense contacts on any link, but would not be able to distinguish among them. By the use of both base force/torque sensing and joint torque sensing it is conceivable to realize a fully sensorized robot surface. A "whole hand" manipulation system, employing intrinsic contact sensors in each phalanx of its three fingers and in the palm, has been designed, and a prototype finger built, as reported by Vassura and Bicchi [1989].

8 Discussion

In this paper we presented material on the mathematics and mechanics of intrinsic contact sensing, and attempted to organize it into a coherent formulation of contact analysis from force measurement. The paper's main contributions are perhaps the introduction of the concept of contact centroid along with the proof of its geometric properties, and the presentation of mathematical methods to compute its location on a sensor surface. In this section we will briefly elaborate on these themes, to underscore some interesting aspects.

The interest of the contact centroid for characterizing soft fingers contacts follows from its property of being located inside the convex hull enclosing every contact point. To illustrate this, a simple numerical example will be worked out. Assume that the real pattern of contact on the surface of a spherical sensor is comprised of only four points $\mathbf{c}_1, \ldots, \mathbf{c}_4$, located on top of the sphere as shown in figure 8, and let $\pm\delta$ and $\pm 8\delta$ be the coordinates along the x-axis of points $\mathbf{c}_1$, $\mathbf{c}_3$, $\mathbf{c}_2$, and $\mathbf{c}_4$ respectively.

Let the local contact forces exerted at these points be $\mathbf{h}_1 = (-h_f, h_f, -1)$, $\mathbf{h}_2 = (-h_f, h_f, -1)$, $\mathbf{h}_3 = (h_f, h_f, -1)$, and $\mathbf{h}_4 = (h_f, h_f, -1)$, respectively. Table 1 gives the x-coordinates of the contact centroid $\mathbf{c}$ (calculated through the algorithm proposed in section 5) and of the point-contact method point $\mathbf{c}'$ (section 4) corresponding to different values of δ and h_f.

As can be seen, the two results diverge as the distance δ and the friction force h_f increase. Note also that for large values of δ the contact centroid retains the characteristic of remaining inside the contact points, while the point obtained by the point-contact method does not.

Another important advantage of the intrinsic contact sensing method is its ability to calculate the local torque originated from friction forces. The importance of these local torques in fine manipulation operations by robot hands has been often underestimated. To appreciate their role, however, it should be considered how humans can hold a stick horizontally by pinching it at one end between two fingertips (with a gripping force of 10N, the fingers can typically resist a torque of 40Nmm and a vertical weight of 5N).

The computational efficiency of the solving algorithms is of paramount importance in real-time applications of intrinsic contact sensing. In table 2 are reported computation times for the same surface, a sphere centered in the origin. The algorithms described in section 6, 4, and 5 have been implemented and timed in a real-time environment running on a Motorola 68030 processor with mathematic coprocessor Motorola 68881. Note that the iterative algorithm is inferior to the other solutions, which are both fast enough to be claimed real-time. Another weakness of the iterative method is that the multiple solutions of equation 17 cannot be discriminated in advance of their actual computation. The iterative algorithm is then recommended only for finding a complete solution for non-ellipsoidal surfaces (e.g. paraboloids) for which closed-form exact methods are not available.

To conclude the comparative analysis of the proposed algorithms, it must be noted that the exact method of section 5 is also preferable to the wrench-axis algorithm from a numerical stability point of view. In fact, as the formulation of the problem in terms of minimization of a quadratic error function given in section 6 shows, the contact problem is intrinsically stable. This is not true of the approximation that disregards local torques. Table 3 shows how small perturbations on the inputs (the force/torque sensor readings $\mathbf{f}$ and $\mathbf{m}$) reflect in small perturbation in the calculated contact point for the method of section 5, while they can lead to inconsistent (complex) results for the wrench-axis method.

Devices based on the force-based contact sensing approach have been actually implemented, and effectively employed in robotic hands. For a discussion on the realization of force/torque sensors on small robot fingertips, see [Brock and Chiu, 1985], and [Bicchi 1987]. The latter paper discusses the application of optimal design techniques to miniaturized force/torque sensors; such approach is expanded in a more thorough treatment in [Bicchi, 1990b].

The applications of intrinsic contact sensors to robotic manipulation are numerous, and several have been experimentally verified. Although it is not possible to detail these applications here, they will be cited for reference:

- The exploration of unknown objects by probing with an intrinsic tactile sensor, and the reconstruction of their surface profile has been described by Brock and Chiu [1985], and later by Tsujimura and Yabuta [1988]. Both authors employed the point-contact method algorithm. Bicchi [1989] reported about explorations performed using the more precise algorithm of section 5, and a hybrid control scheme, which allowed continuous control of the normal component of contact force.

- The capability of intrinsic contact sensors to evaluate the friction components of the contact force and the local torque (which is unique among other available sensing devices), has been used to measure the coefficients of friction of various objects [Bicchi, 1989]. This information in turn has been used to discriminate objects on the basis of their apparent friction, and to plan subsequent slippage-safe operations of the hand.

- A real-time control method for augmenting the stability of the grasp of unmodeled objects against slippage has been discussed and demonstrated (in a rather simple setting) by Bicchi, Salisbury and Dario [1989].

The exploitation of contact sensory information is expected to allow improvements in many areas of fine manipulation control. Contact sensors such as those described in this paper can provide direct, real-time and reliable feedback of fundamental contact interaction characteristics. For instance, intrinsic contact sensors could be profitably used to improve the accuracy of the control of micro-motions of manipulated objects or tools, especially in the presence of slipping and/or rolling contacts.

Acknowledgments

The authors would like to gratefully acknowledge the financial support from the following sources: the Systems Development Foundation, NASA contract number NAG-9-319, Sandia National Laboratories under contract 75-2608, the Office of Naval Research University Research Initiative Program under Office

of Naval Research contract N00014-86-K-0685, the Advanced Research Projects Agency of the Department of Defense under Office of Naval Research contract N00014-85-K-0124, and the Consiglio Nazionale delle Ricerche, Progetto Finalizzato Robotica. Support for Antonio Bicchi at the M.I.T Artificial Intelligence Laboratory has been granted through the NATO-CNR joint fellowship n.215.22/07.

References

Balestrino, A., De Maria, G., and Sciavicco, L. 1984. Robust Control of Robotic Manipulators.*Proc. 9th IFAC World Congress* vol.6, pp.80-85.

Bicchi, A. 1989. Strumenti e Metodi per il Controllo di Mani per Robot. Ph.D. thesis, Universitá di Bologna, Dept. of Mechanical Engineering.

Bicchi, A. 1990. Intrinsic Contact Sensing for Soft Fingers. *Proc. IEEE Int. Conf. Robotics and Automation.* Cincinnati, OH: pp. 968-973.

Bicchi, A. 1990b. A Criterion for the Optimal Design of Multi-Axis Force Sensors. *MIT AI Lab Memo 1263.* Cambridge, MA: Artificial Intelligence Laboratory, Massachusetts Institute of Technology.

Bicchi, A., Dario, P. 1987. Intrinsic Tactile Sensing for Artificial Hands. *Proc. 4th Int. Symp. on Robotics Research* Santa Barbara, CA.: R. Bolles and B. Roth Editors, MIT Press, Cambridge, MA. pp.83-90.

Bicchi, A., Salisbury, J.K., Dario, P. 1989. Augmentation of Grasp Robustness Using Intrinsic Tactile Sensing. *Proc. IEEE Conf. on Robotics and Automation.* Scottsdale, AZ: IEEE, pp.302-307.

Brock, D.L, and Chiu, S. 1985. Environment Perceptions of an Articulated Robot Hand Using Contact Sensors. *Proc. ASME Winter Annual Meeting.* Miami, FL: pp 228-235.

Dahlquist, G., and Björk, rA. 1974. *Numerical Methods.* Prentice Hall.

Das, H., Slotine, J.-J.E., and Sheridan, T.B. 1988. Inverse Kinematic Algorithms for Redundant Systems. *Proc. IEEE Int. Conf. on Robotics and Automation.* Philadelphia, PA: IEEE, pp.43-48.

Eberman, B. S. and Salisbury, J.K. 1990. Determination of Manipulator Contact Information from Joint Torque Measurements.*Lecture Notes in Control and Information Sciences.* Hayward, V. and O. Khatib (Eds.), Springer-Verlag, New York, NY.

Howe, R. D. and Cutkosky, M. R. 1992. Touch Sensing for Robotic Manipulation and Recognition. *Robotics Review 2.* O. Khatib and et al., MIT Press, Cambridge, MA.

Hunt, K.H. 1978. *Kinematic Geometry of Mechanisms.* Oxford University Press, London, U.K.

Johnson, K.L. 1985. *Contact Mechanics.* Cambridge University Press, London, U.K.

Mason, M.T. and Salisbury, J.K. 1985. *Robot Hands and the Mechanics of Manipulation.* MIT Press, Cambridge, MA, USA.

Minsky, M.: Manipulator Design Vignettes. *MIT AI Lab Memo 267, 1972*, re-issued as *MIT AI Lab Memo 267A, 1981.* Cambridge, MA: Artificial Intelligence Laboratory, Massachusetts Institute of Technology.

Nicholls, H.R. and Lee, M.H. 1989. A Survey of Robot Tactile Sensing Technology. *Int. Jour. Robotics Research*, Vol 8, No. 3, pp. 3-30.

Okada, T. 1990. A new Tactile Sensor Design Based on Suspension-Shells. *Dextrous Robot Hands*, Venkataraman, S.T., and Iberall, T., eds. Springer-Verlag, New York, NY.

Peronneau, G.: Position-Indicating System, *US patent Number 3,657,475*, April 1972.

Press, W.H., Flannery, B.P., Teukolsky, S.A., Vetterling, W.T. 1988. *Numerical Recipes in C*, Cambridge University Press, London, U.K.

Salisbury, J. K. 1983. Kinematic and Force Analysis of Articulated Hands. Ph.D. Thesis, Stanford University.

Salisbury, J.K. 1984. Interpretation of Contact Geometries from Force Measurements. *Proc. 1st Int. Symp. on Robotics Research*, M.Brady and R.Paul (eds.). Bretton Woods, N.H.: MIT Press, Cambridge. pp. 565-577.

Tsujimura, T., and Yabuta, T. 1988. Object Detection by Tactile Sensing Method employing Force/Torque Information. *IEEE Trans. on Robotics and Automation.* Vol. 5, no. 4.

Vassura, G. and Bicchi, A. 1989. Whole Hand Manipulation: Design of an Articulated Hand Exploiting All Its Parts to Increase Dexterity. *Robots and Biological Systems*, NATO-ASI Series, Springer-Verlag, New York, N.Y.

Whitney, D.E.: "Historical Perspective and State of the Art in Robot Force Control," International Journal of Robotics Research, vol.6, No.1, Spring 1987.

Appendix 1.

The contact centroid general property given in section 2.1 will be proved in three steps, where properties of increasing generality are illustrated.

> **Property 1:** If a distribution Δ of compressive contact tractions $\mathbf{v}(\mathbf{r})$, acts on a set of contact points $C = \{\mathbf{r}_c\}$ of a planar surface $P(\mathbf{r}) = 0$, the contact centroid of Δ on P lies inside the convex hull enclosing every point $\mathbf{r}_c$ (see figure 9).
>
> **Proof:** Consider a line ρ on the contact plane P passing through at least one contact point $\mathbf{r}_c$ and leaving all others on the same half plane, as depicted in figure 9. By definition 1, a set of forces equivalent to the given contact set is comprised of a resultant force $\mathbf{p} = \int_P \mathbf{v}(\mathbf{r})$ applied at the contact centroid, and a torque $\mathbf{q}$ normal to the contact plane. In order to satisfy the balance of moments about the line ρ, the contact centroid must lie on the same half plane where the contact points do. Considering the family of all such lines ρ, the convex hull results as the envelope of the family, and the thesis follows.

In other words, for a planar sensor with compressive forces, no matter how far away the contact points are from each other, the contact can be considered "soft finger," and the contact centroid lies inside the smallest convex polygonal line enclosing every contact point.

> **Property 2:** Consider a convex surface $S(\mathbf{r}) = 0$ (see figure 10), and a plane $P(\mathbf{r}) = 0$ intersecting S. Let $\mathbf{n}'$ be the normal unit vector to P, pointing at the half space where $P(\mathbf{r}) > 0$). Assume that a distribution Δ of contact tractions $\mathbf{v}(\mathbf{r})$ is exerted on a set C of points $\mathbf{r}_c$ lying on P and internal to S , and assume that the tractions are compressive with respect to $\mathbf{n}'$ (i.e., $\mathbf{n}'^T\mathbf{v}(\mathbf{r}_c) < 0$, for all $\mathbf{r}_c$). In these hypotheses, the contact centroid of Δ on S lies in the half space $P(\mathbf{r}) > 0$.
>
> **Proof:** Because of the first property of contact centroids, the distribution Δ of contact forces applied on C is equivalent to its resultant force $\mathbf{p}$ applied to a contact centroid $\mathbf{c}'$ on P, and torque $\mathbf{q}'$, such that $\mathbf{c}'$ is inside S and $\mathbf{q}'$ is parallel to $\mathbf{n}'$. We denote with $\mathbf{c}$, $\mathbf{n}$ and $\mathbf{q}$ the contact centroid of Δ on S, the associated normal, and the local torque, respectively. Let $\mathbf{e} = \mathbf{c} - \mathbf{c}'$. The balance of moments about $\mathbf{c}'$ can then be written as

$$\mathbf{q}' = \mathbf{q} + \mathbf{e} \times \mathbf{p}, \tag{18}$$

which can be rewritten as

$$\xi'\mathbf{n}' = \xi\mathbf{n} + \mathbf{e} \times \mathbf{p}, \tag{19}$$

where ξ and ξ' are scalar constants. By multiplying both members of equation 19 by $\mathbf{p}^T$, and by $\mathbf{e}^T$, we obtain two equations,

$$\xi'\mathbf{p}^T\mathbf{n}' = \xi\mathbf{p}^T\mathbf{n}, \tag{20}$$

$$\xi'\mathbf{e}^T\mathbf{n}' = \xi\mathbf{e}^T\mathbf{n}. \tag{21}$$

From the hypotheses above and from the definition of contact centroid, $\mathbf{p}^T\mathbf{n}' < 0$ and $\mathbf{p}^T\mathbf{n} < 0$ (compressive contact). Hence, from equation 20, ξ and ξ' must have the same sign or be both zero.

If ξ and ξ' are not null and have the same sign, equation 21 implies that $\mathbf{e}^T\mathbf{n}'$ and $\mathbf{e}^T\mathbf{n}$ also have the same sign. Since S is convex and $\mathbf{c}'$ is inside S, $\mathbf{e}^T\mathbf{n} > 0$ for every $\mathbf{e}$. Therefore, $\mathbf{e}^T\mathbf{n}' > 0$, that is $\mathbf{e}$ points to the half space $P(\mathbf{r}) > 0$, that was the thesis.

Otherwise, if both ξ and ξ' are zero, than from equation 19 follows that $\mathbf{e}$ and $\mathbf{p}$ must be parallel. Let $\mathbf{e} = \zeta\mathbf{p}$. Again using the fact that $\mathbf{p}^T\mathbf{n} < 0$ (definition of contact centroid) and $\mathbf{e}^T\mathbf{n} = \zeta\mathbf{p}^T\mathbf{n} > 0$ (convexity of S), we have that $\zeta < 0$. Since $\mathbf{c}'$ is a contact centroid, $\mathbf{p}^T\mathbf{n}' < 0$. Finally we have $\mathbf{e}^T\mathbf{n}' = \zeta\mathbf{p}^T\mathbf{n}' > 0$, q.e.d..

Rephrased, this second property has some intuitive meaning. Consider a sensor with convex, compliant surface which is deformed by contact with a flat object. No adhesive forces are exerted, and the deformed surface stays inside the undeformed one. Since the deformed surface is not known, the contact centroid can only be calculated relative to the sensor's undeformed surface. However, the contact centroid is well behaved, in the sense that it will stay on the same side of the areas being touched (see figure 10).

Property 3: Consider a deformable body, whose undeformed surface $S(\mathbf{r}) = 0$ is convex, and assume that a distribution Δ of compressive contact tractions is exerted on a set of contact points $C = \{\mathbf{r}_c\}$ of S. Consider a plane $P(\mathbf{r}) = 0$ that divides the surface of the deformed body in two portions, so that every contact point is confined in one half-space (see figure 2). Consider the projection of each contact point $\mathbf{r}_c$ on P along the direction of the traction applied at $\mathbf{r}_c$. If all such projections lie inside the undeformed surface S, then the contact centroid on S of Δ lies on the same side of P where Δ is applied.

Proof: Since pure forces or tractions can be moved along their line of application without affecting the resultant force and torque of the set, this proposition is easily derived from property 2.

In order to give the best estimate of the location of contact points, the plane P can be chosen as the one that separates the smallest portion of S enclosing every contact point/area. If some contact points belong to P, it is required that the contact traction at those points be strictly compressive with respect to the plane.

Appendix 2.

Proposition 2: Uniqueness of Solutions

A solution to the contact sensing problem, described by equations 1 through 4 and by the definition of contact centroid, is unique (if it exists), if and only if the surface is convex.

Proof: The "if" part of the proposition can be demonstrated by contradiction. Assume that there are two points, $\mathbf{c}$ and $\mathbf{c}'$, expressed in an arbitrary reference frame B, lying on a convex surface S and which are solutions of the contact sensing problem. Consider the vector $\mathbf{e} = \mathbf{c}' - \mathbf{c}$, as shown in figure 11. Because of the surface convexity we have

$$\begin{aligned} \mathbf{e}^T \mathbf{n}' &> 0, \\ \mathbf{e}^T \mathbf{n} &< 0. \end{aligned} \tag{22}$$

The balance of moments at point $\mathbf{c}$ can be written as

$$\mathbf{q} = \mathbf{q}' + \mathbf{e} \times \mathbf{p},$$

Since $\mathbf{q}$ and $\mathbf{q}'$ are parallel to $\mathbf{n}$ and $\mathbf{n}'$ respectively, we can rewrite

$$\xi \mathbf{n} = \xi' \mathbf{n}' + \mathbf{e} \times \mathbf{p}, \tag{23}$$

and, by multiplying both terms by $\mathbf{p}^T$, we have

$$\xi \mathbf{p}^T \mathbf{n} = \xi' \mathbf{p}^T \mathbf{n}',$$

Since forces are assumed compressive, this implies that either $\xi\xi' > 0$ or $\xi = \xi' = 0$.

If $\xi = \xi' = 0$, no local torques are exerted at $\mathbf{c}$ nor at $\mathbf{c}'$, and those points lie on a line parallel to $\mathbf{p}$. Because of the convexity of S, only one of the two intersections of such a line can satisfy the definition of contact centroid ($\mathbf{p}^T \mathbf{n} < 0$).

If $\xi\xi' > 0$, we multiply both terms of equation 23 by $\mathbf{e}^T$, and obtain

$$\xi \mathbf{e}^T \mathbf{n} = \xi' \mathbf{e}^T \mathbf{n}'.$$

Together with the convexity condition 22, this implies that either $\xi\xi' < 0$ which is a contradiction, or that $\mathbf{e} = 0$, which is the thesis. In addition, it can be shown that the uniqueness of the contact centroid holds if the surface is planar, provided that the contact tractions are strictly compressive.

To demonstrate the "only if" part, suppose the surface is not convex as in figure 12. Suppose there exists two distinct points such that

$$\begin{aligned} \mathbf{e}^T \mathbf{n}' &< 0, \\ \mathbf{e}^T \mathbf{n} &< 0. \end{aligned} \tag{24}$$

Thus a compressive force in the direction of $\mathbf{e}$ applied at either point yields identical sets of forces and moments. Hence the solution is not unique and the statement is proved.

Footnotes List

1. The *wrench axis* is a generalization of the concept of a line of action of a force. When an arbitrary set of forces and torques acts on a body, they may be described canonically by a unique line along which a unique force acts, together with a unique moment exerted about the line (see [Hunt, 1978]).

2. The term *traction* [Johnson,1985] indicates a force per surface unit, comprised in general of a normal component (pressure) and tangential (friction) component.

3. We will show in section 3 that for convex surfaces the contact centroid is actually unique.

4. The concept of a contact centroid was not explicit in the initial definition of the soft finger contact given by Salisbury [1983]; that was based on an assumption of very small contact area. The contact centroid introduced by Bicchi [1989] allows for a broader applicability of the soft finger contact type. It should be noted that for flat surfaces, the contact centroid coincides with the center of friction introduced by Mason [Mason and Salisbury, 1985].

Captions for Figures

1. Simple contact sensing.
2. The contact centroid has the property of being close to the actual contact area.
3. A spherical sensor surface with friction coefficient $\mu = \tan\varphi$.
4. Vector quantities and notation involved in the problem statement.
5. The fingertip sensors of the Salisbury Robot Hand are composed of a hemisphere on top of a cylinder.
6. A compound sensor surface with corners and edges.
7. Fully sensorized robot arms can be constructed in principle using only force/torque measurements.
8. A simple contact pattern used as an example.
9. Contact on a planar surface.
10. Contact on a deformable surface.
11. The contact centroid on a convex surface is unique.
12. Concave surfaces may have non-unique contact centroids.

Captions for Tables

1. Position of the contact centroid $\mathbf{c}$ and of the approximated (wrench-axis method) point $\mathbf{c}'$ along the x-axis for different values of δ and h_f.

2. Computation times for the three algorithms to solve the contact problem on a sphere. The iterative method takes an average of 20 steps to converge under 1e-6 error when input data are slowly varying.

3. Algorithm sensitivity analysis. Noise on the measurement of the second component of the measured moment $\mathbf{m}$ is simulated. The centroid is computed for a unit radius sphere. Question marks indicate inconsistent (complex) results.

Figures

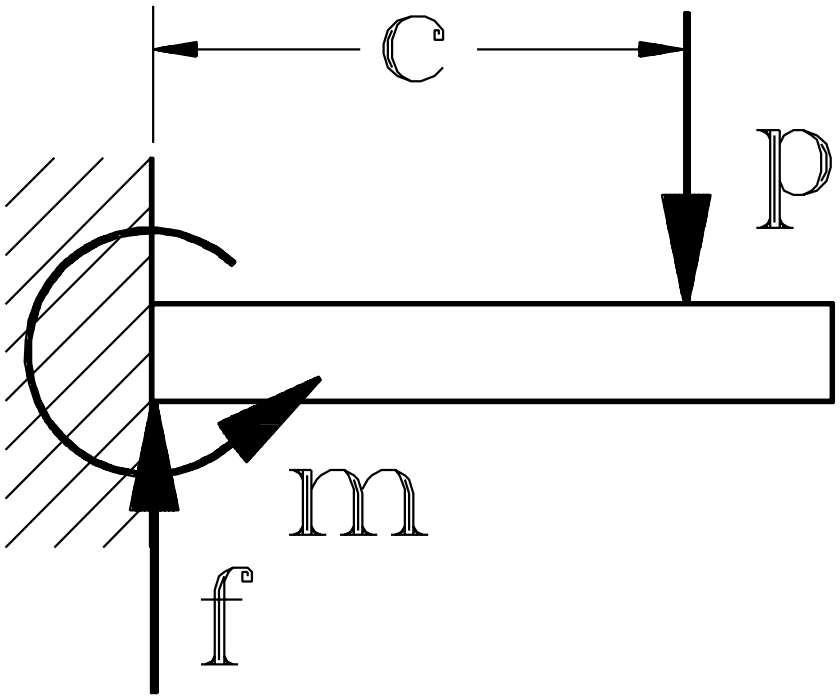

Figure 1

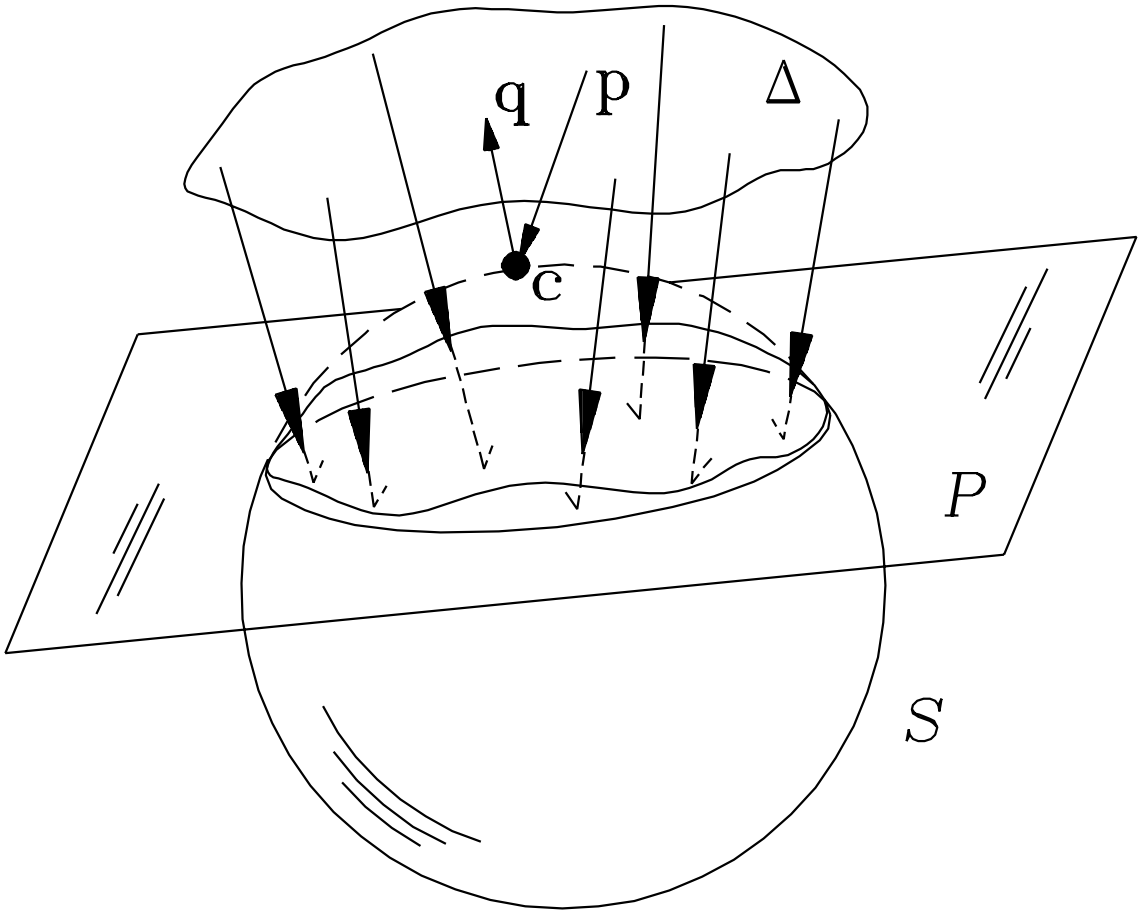

Figure 2

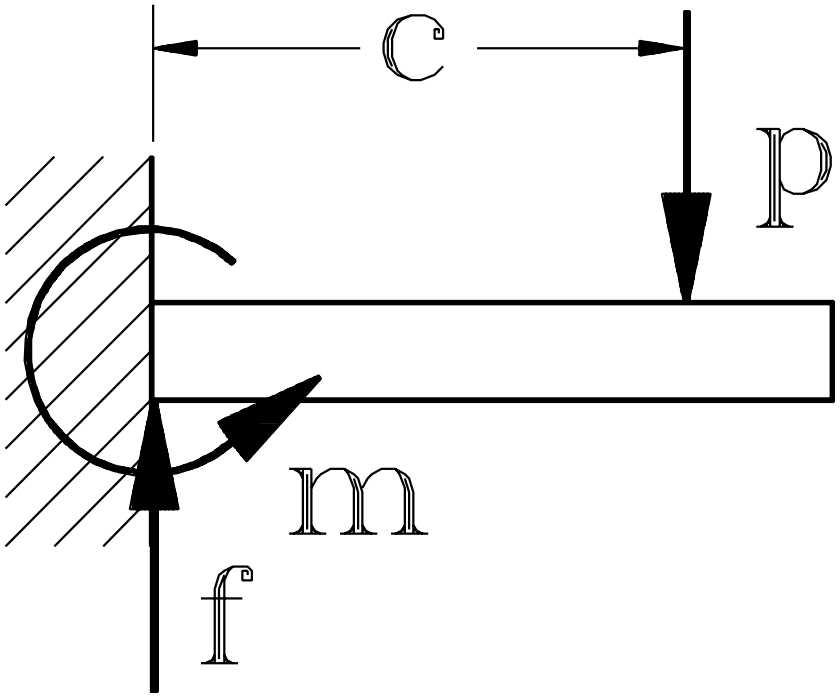

Figure 1

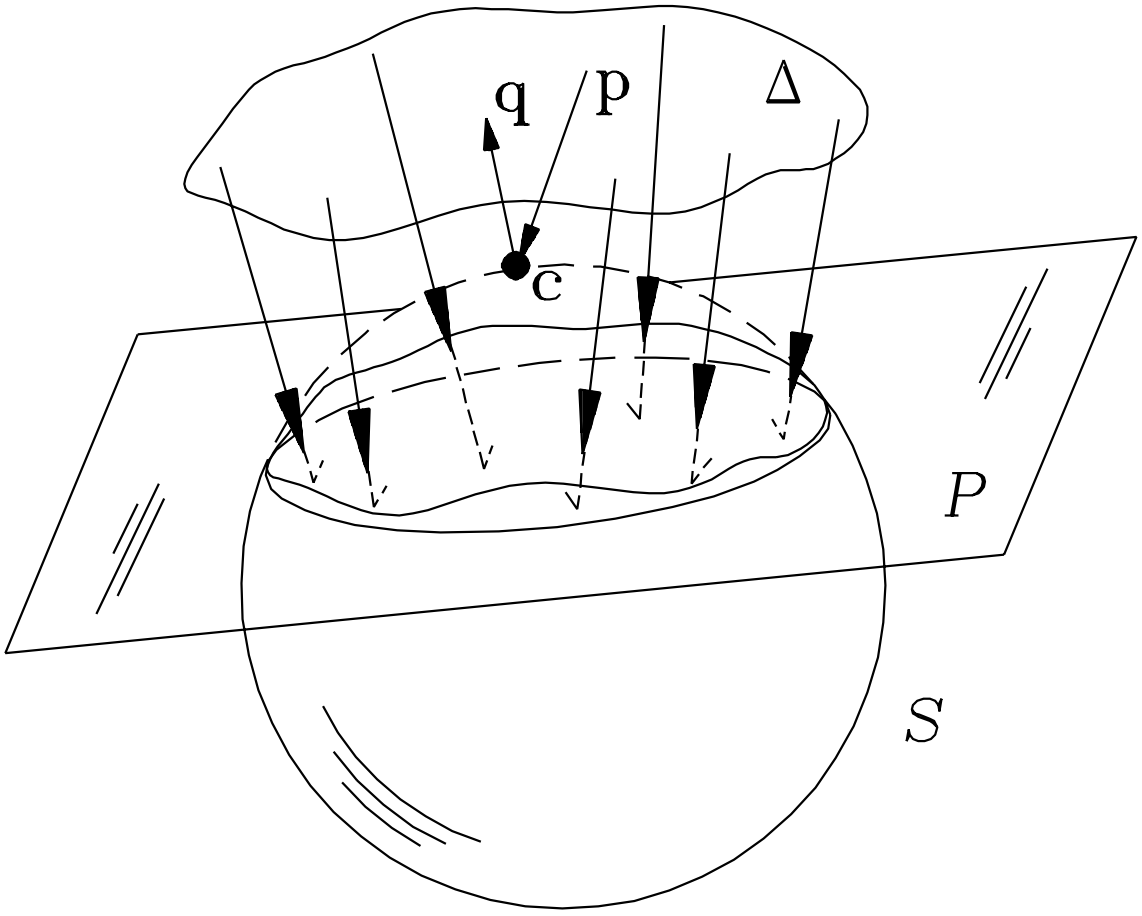

Figure 2

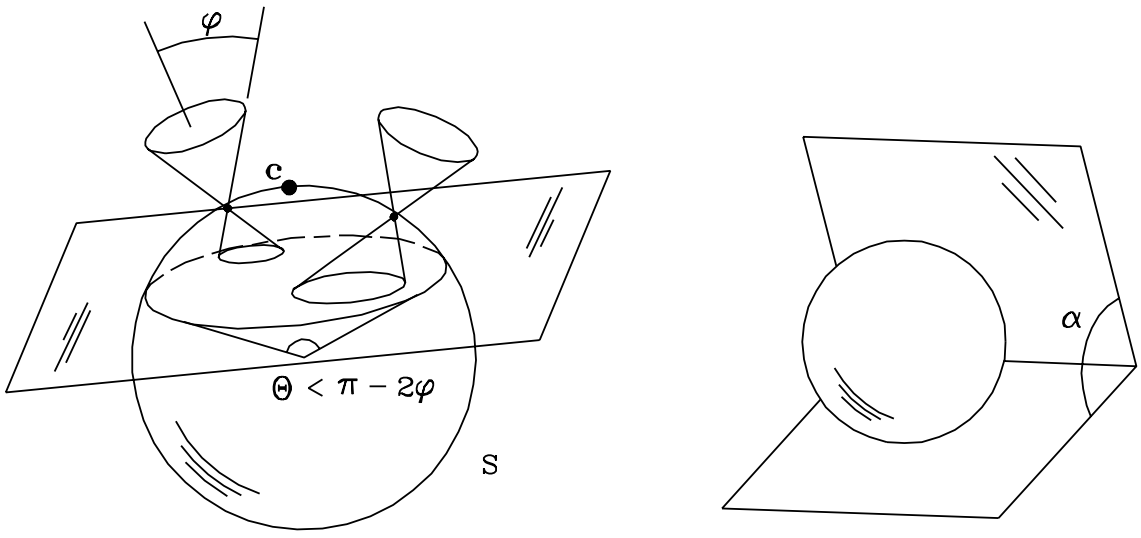

Figure 3

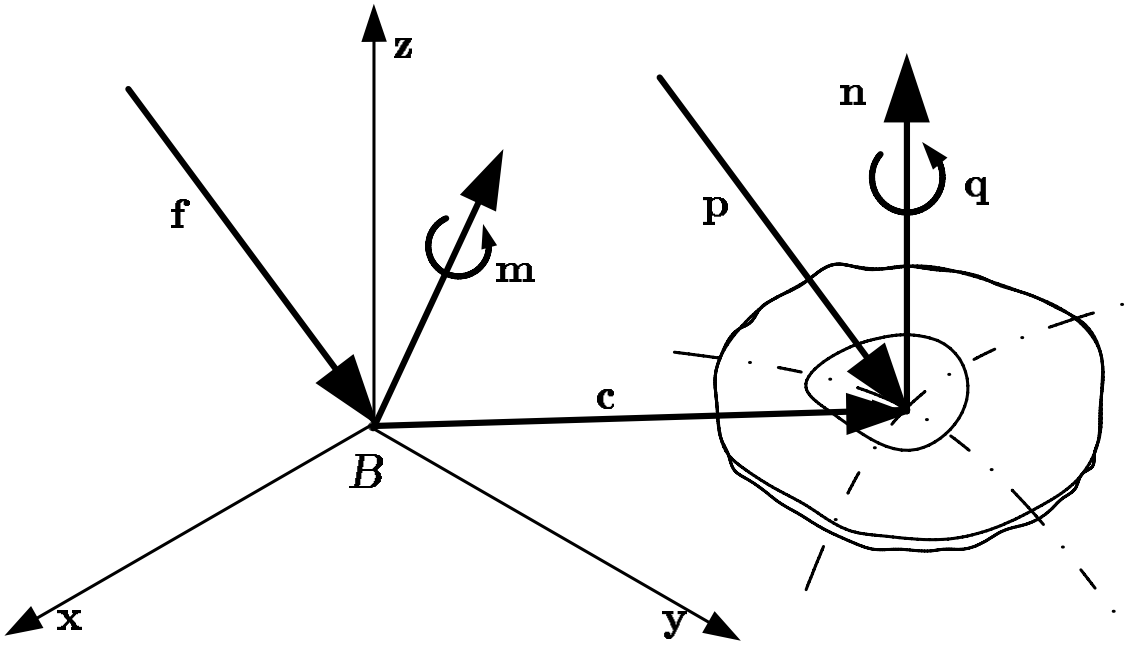

Figure 4

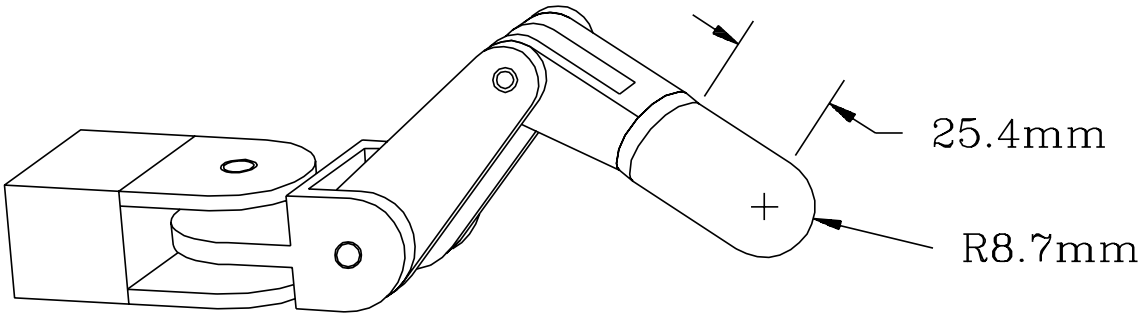

Figure 5

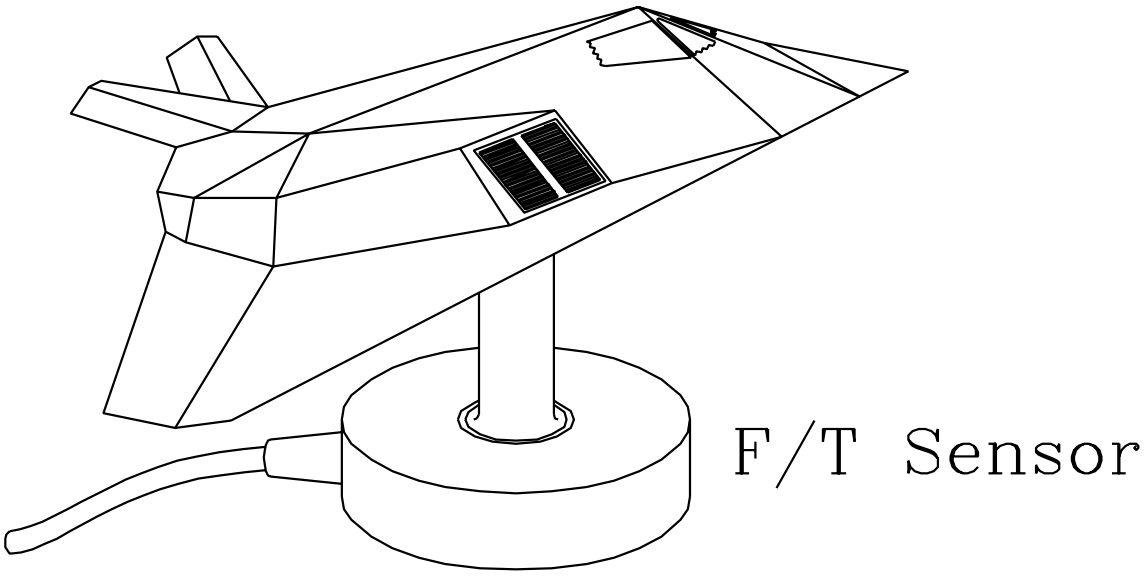

Figure 6

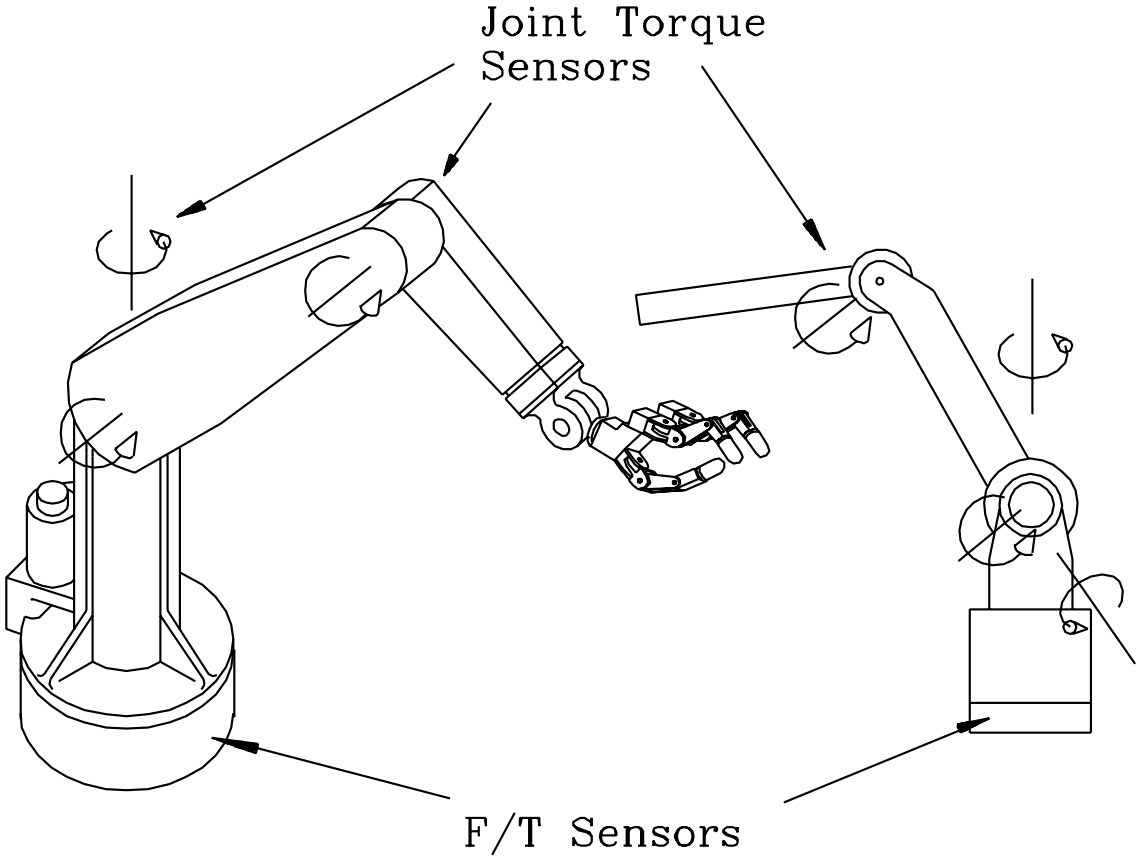

Figure 7

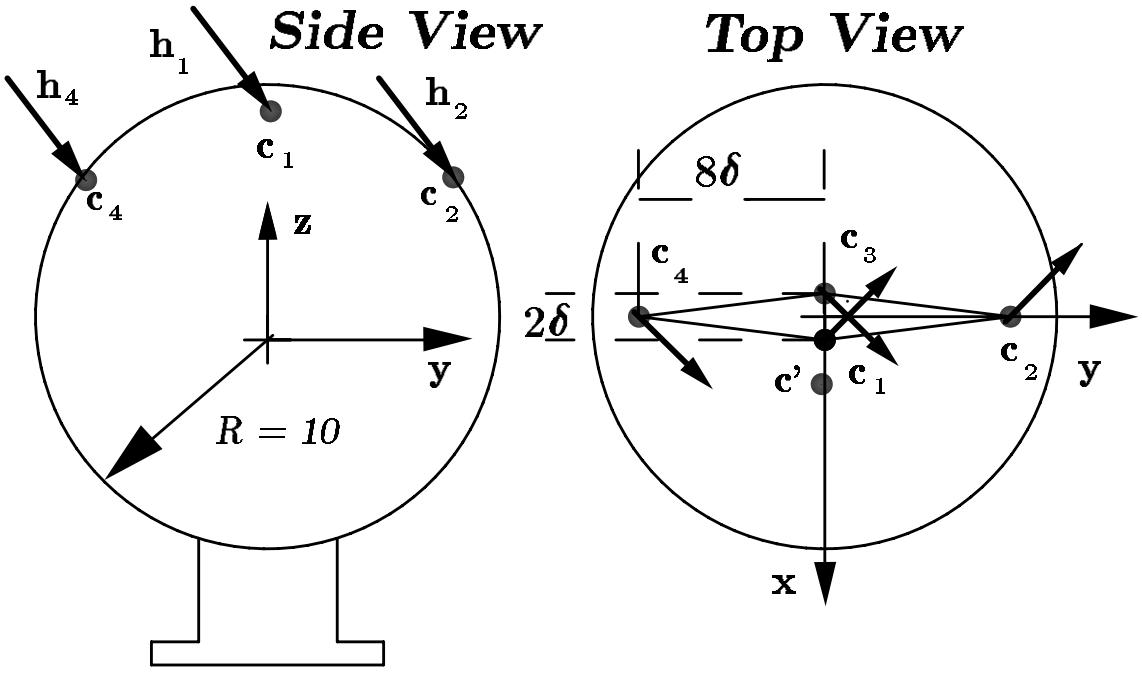

Figure 8

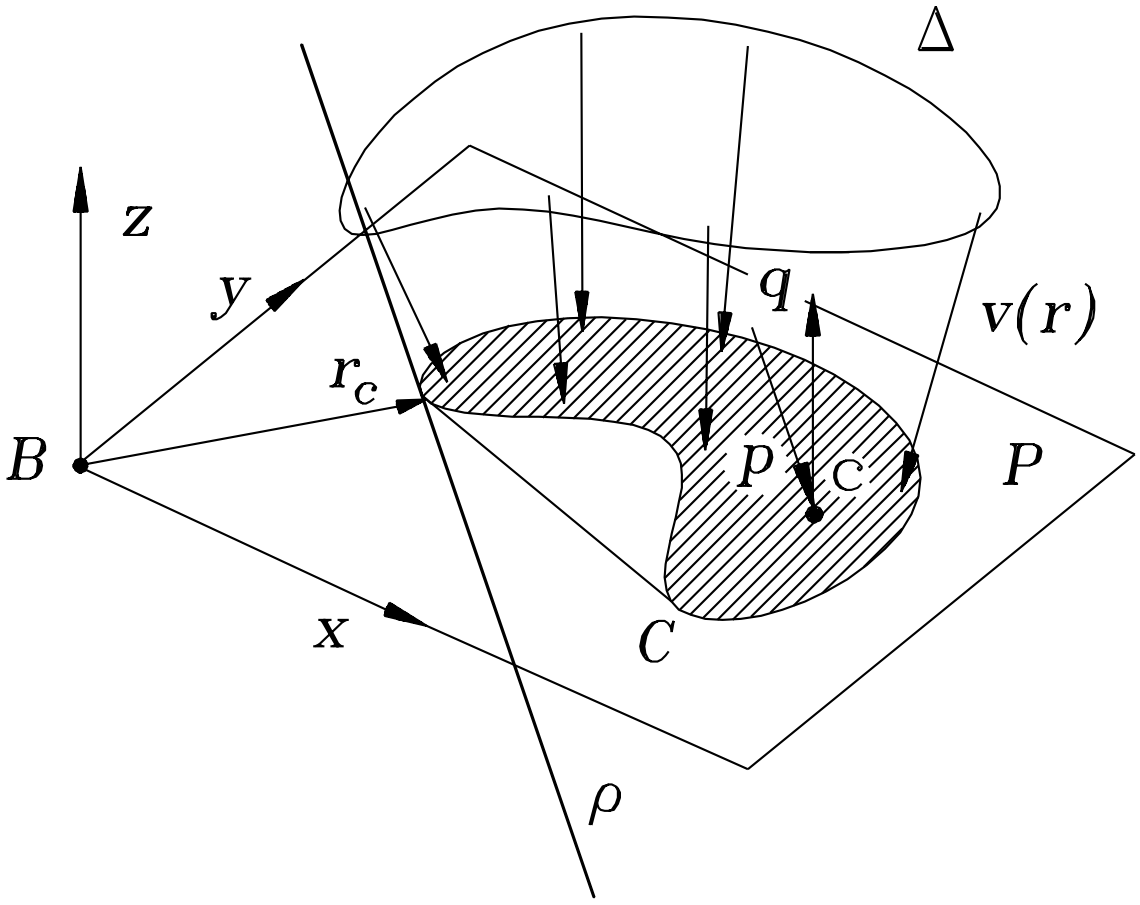

Figure 9

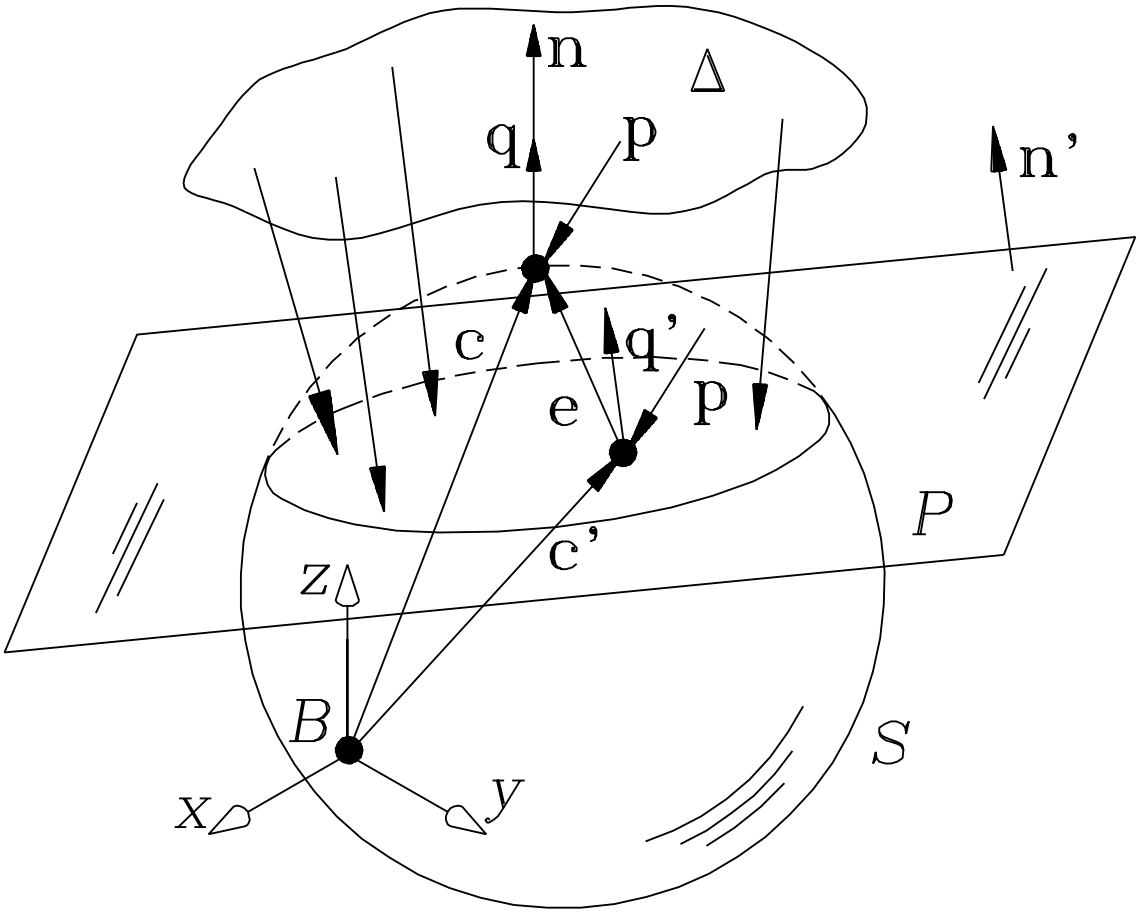

Figure 10

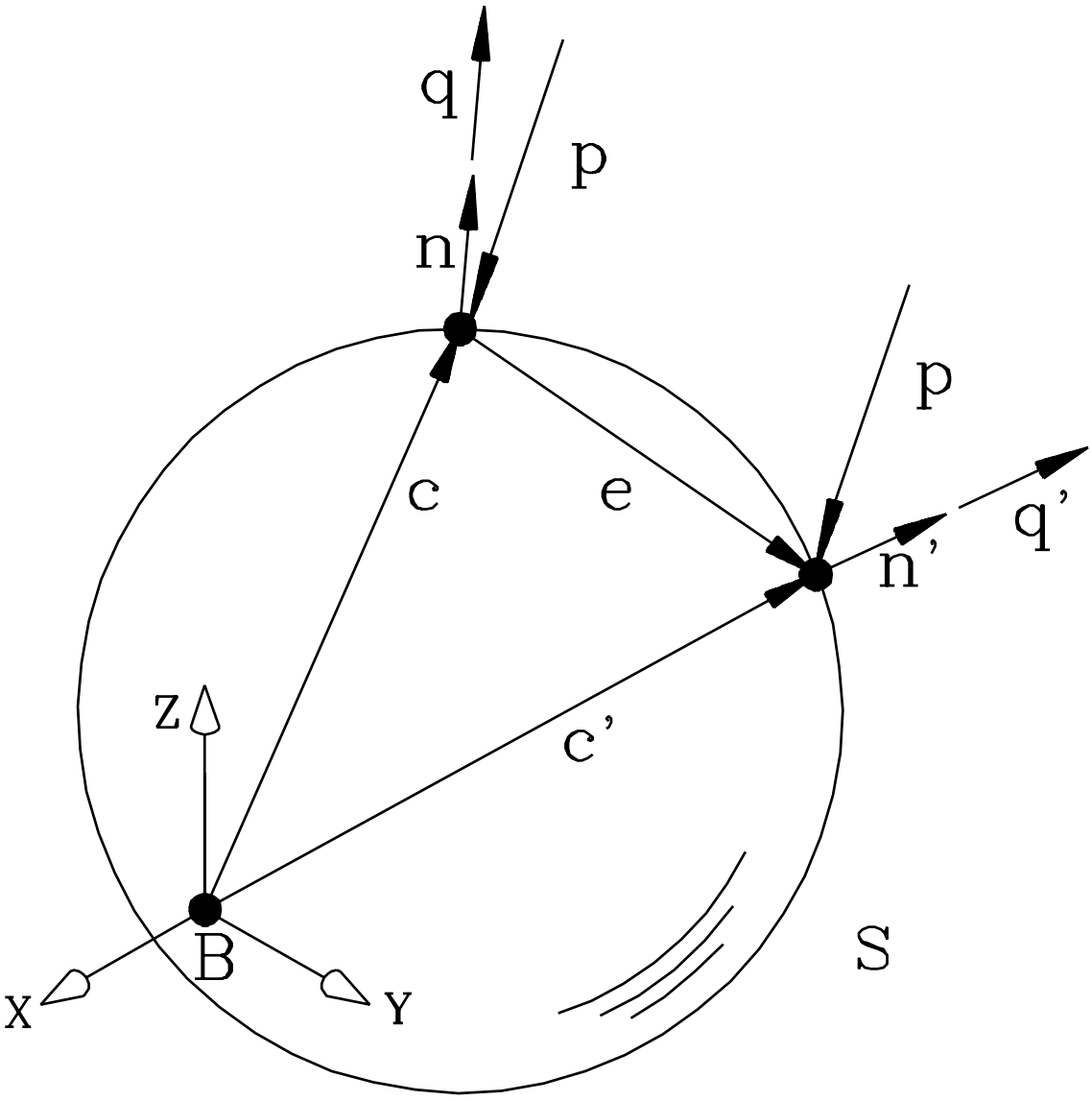

Figure 11

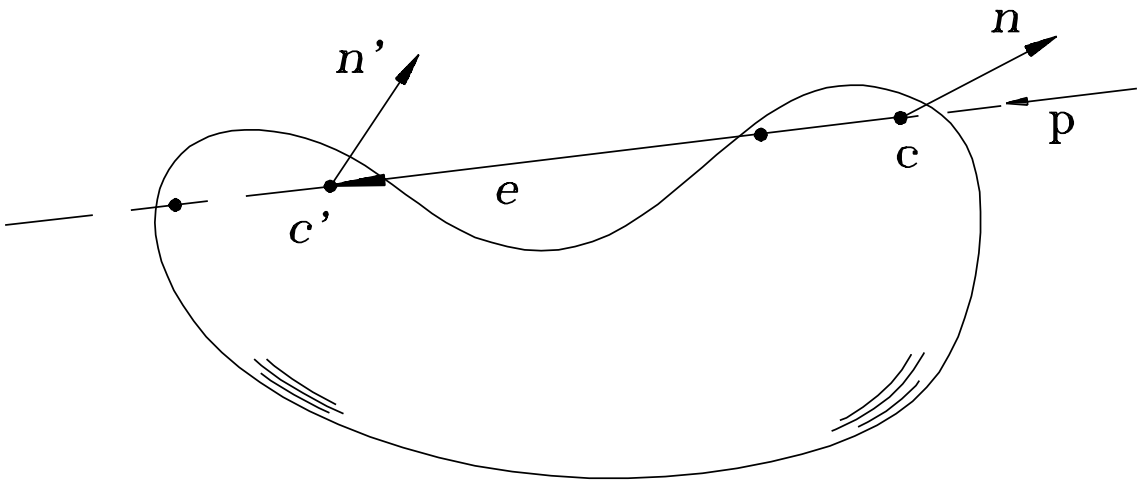

Figure 12

Tables

δ / h_f	0.125	0.25	0.5
0.1	c_x : 0.000	c_x : 0.000	c_x :0.000
	c'_x : 0.005	c'_x : 0.010	c'_x : 0.020
0.7	c_x : 0.000	c_x :0.005	c_x :0.039
	c'_x : 0.164	c'_x : 0.329	c'_x :0.658
1	c_x : 0.001	c_x :0.010	c_x :0.077
	c'_x : 0.250	c'_x : 0.500	c'_x :1.000

Table 1

	Iterative Method	Wrench-Axis Method	Ellipsoid Method
Execution time	473±13 μsec/step	232±6 μsec	486±13 μsec

Table 2

Method F/T Measurements	Iterative	Wrench-Axis	Ellipsoid
$\mathbf{f}$ = [-0.3 -.04 0.01] $\mathbf{m}$ = [0.01 0.01 0.48]	$\mathbf{c}$ = [-0.60 0.80 0.00]	$\mathbf{c}'$ = [-0.60 0.80 0.00]	$\mathbf{c}$ = [-0.60 0.80 0.00]
$\mathbf{f}$ = [-0.3 -.04 0.01] $\mathbf{m}$ = [0.01 0.01 0.49]	$\mathbf{c}$ = [-0.66 0.75 0.04]	$\mathbf{c}'$ = [-0.66 0.75 0.00]	$\mathbf{c}$ = [-0.66 0.75 0.04]
$\mathbf{f}$ = [-0.3 -.04 0.01] $\mathbf{m}$ = [0.01 0.01 0.50]	$\mathbf{c}$ = [-0.73 0.68 0.07]	$\mathbf{c}'$ = [? ? ?]	$\mathbf{c}$ = [-0.74 0.67 0.09]
$\mathbf{f}$ = [-0.3 -.04 0.01] $\mathbf{m}$ = [0.01 0.01 0.51]	$\mathbf{c}$ = [-0.76 0.62 0.20]	$\mathbf{c}'$ = [? ? ?]	$\mathbf{c}$ = [-0.76 0.62 0.20]

Table 3